

Original

Lemos, G.; Fredel, M.; Pyczak, F.; Tetzlaff, U.:

Influence of Distinct Manufacturing Processes on the Microstructure of Ni-Based Metal Matrix Composites Submitted to Long Thermal Exposure.

In: Key Engineering Materials. Vol. 809 (2019) 79 - 86.

First published online by Trans Tech Publications: June, 2019

DOI: 10.4028/www.scientific.net/KEM.809.79

<https://dx.doi.org/10.4028/www.scientific.net/KEM.809.79>

Influence of Distinct Manufacturing Processes on the Microstructure of Ni-Based Metal Matrix Composites Submitted to Long Thermal Exposure

Georges Lemos^{1,a*}, Márcio C. Fredel^{2,b},
Florian Pyczak^{3,4,c} and Ulrich Tetzlaff^{1,d}

¹Technische Hochschule Ingolstadt, 85049 Ingolstadt, Germany

²Universidade Federal de Santa Catarina, 88040-900 Florianopolis, Brazil

³Brandenburgische Technische Universität Cottbus-Senftenberg, 03013 Cottbus, Germany

⁴Helmholtz-Zentrum Geesthacht, 04152 Geesthacht, Germany

^aGeorges.Lemos@thi.de, ^bM.Fredel@ufsc.br, ^cFlorian.Pyczak@hzg.de, ^dUlrich.Tetzlaff@thi.de

*corresponding author

Keywords: MMC, particle reinforcement, TiC, isothermal aging, superalloy, Inconel X-750.

Abstract. Metal Matrix Composites (MMCs) are known for their remarkable properties, by combining materials from different classes. Ni-based MMCs are a promising group of heat-resistant materials, targeting aerospace applications. A discontinuously reinforced Inconel X-750/TiC 15 vol.% MMC was proposed for use in lighter, creep resistant turbine elements, with the aim to endure service temperatures up to 1073 K (800 °C). However, their microstructural stability at high temperatures for long periods of time remained to be further investigated. To address this need, specimens were produced by both conventional hot pressing and spark plasma sintering, using powders milled by low and high energy processes, followed by long isothermal aging. The treatments were conducted at 973 and 1073 K, for times between 50 and 1000 hours. The resulting samples were investigated with XRD and EDS techniques for phase analysis. In addition, measurements of hardness were made to monitor changes in mechanical behavior. It was found that, for each different manufacturing process, the amount, distribution and size of γ' and other precipitates notably vary during the overaging process. Consequently, the amount of elements kept in solid solution also shifted with time. Furthermore, the study shows how distinct initial microstructures, resulting from diverse fabrication processes, differently impact the microstructural stability over long times of exposure to high temperatures.

Introduction

A new metal matrix composite concept, based on a polycrystalline Ni-based Inconel X-750 superalloy, was proposed as a creep resistant material for turbine elements [1]. To further investigate the microstructure and stability at high temperatures, specimens reinforced with 15 vol.% TiC particles were produced by two different manufacturing routes: one by a low energy milling process, followed by uniaxial press sintering, and other through high energy milling [2], combined with spark plasma sintering. Targeting work temperatures up to 1073 K, the material was submitted to long isothermal treatments, to investigate the microstructure evolution through time.

Milling and Sintering Processes. The combination of two processes, mechanical alloying and Spark Plasma Sintering (SPS), enabled the development of promising new materials in the last few decades. Mechanical alloying is a high energy ball milling process, suitable for the production of fine, homogeneous composite microstructures, already employed with success to reinforce superalloys with oxide particles. What differentiates a high energy from a low energy process, is that in the former the collisions between metallic powders lead to cold welding, before the powders are broken into smaller metallic fragments [2]. Likewise, as an alternative to the traditional pressure sintering, the SPS process also captured interest in the recent decades. This process allows the creation of highly densified materials through a rapid and economical manufacturing route [3]. However, under certain circumstances it may produce temperature gradients that impact the microstructure homogeneity [4].

Phases Evolution During Overaging. During long times of exposure to high temperatures, γ' particles may change in volume and morphology [5]. Likewise, during the overaging process a high content of niobium can also induce the formation of the MC phase in some Ni-based alloys, which might lead to the development of γ' - and γ'' -free zones around the carbides [6, 7]. Additionally, high levels of Ti in the Inconel X-750 can induce the formation of η phase (Ni_3Ti , *eta*), after long times at high temperatures. This phase derives directly from γ' , having a plate-like form. It is frequently located at grain boundaries, reducing their mobility. In addition to a potential loss of ductility, the presence of η phase also leads to the formation of γ' -depleted zones [8].

Materials and Methods

As summarized in Table 1, two non-reinforced Inconel X-750 (composition in Table 2) variants were tested as references: a commercially available alloy, provided as hot-rolled bars, as well as spark plasma sintered (SPS) specimens. Two composites were also produced through powder metallurgy routes, adding 15 vol.% TiC particles as reinforcing phase: one prepared by uniaxial pressure sintering (PS), and a second by SPS technique. The unprocessed powders of Inconel X-750 presented a granulometry of $d_{80} = 22 \mu\text{m}$, while TiC particles exhibited $d_{80} = 3.7 \mu\text{m}$. The combined powders were subjected to low and high energy milling [2] before the PS and SPS processes, respectively. The low energy process was conducted with a Turbula T2F mixer for 15 minutes, while for the high energy process a planetary mill Pulverisette 6 using Fe-Cr-Ni grinding balls was employed for several hours, including periodic breaks to keep the powder temperature under 333 K (60 °C). The milling was conducted under Argon atmosphere.

Table 1 - Materials variants and corresponding processes codes.

Material	Powder Comminution	Production Method
Inconel X-750 non-reinforced	—	Hot-rolling
Inconel X-750/TiC _p 15 vol.%	Low Energy Milling (LEM)	Pressure Sintering (PS)
Inconel X-750 non-reinforced	High Energy Milling (HEM)	Spark Plasma Sintering (SPS)
Inconel X-750/TiC _p 15 vol.%	High Energy Milling (HEM)	Spark Plasma Sintering (SPS)

Table 2 - Chemical composition (wt.%) of Inconel X-750.

Element	Cr	Fe	Ti	Nb	Al	Si	Mn	Co	C	Cu	S	N
Wt. %	15.3	6.5	2.71	1.1	0.7	0.2	0.1	0.03	0.02	0.01	0.003	bal.

After production, the material was submitted to a triple heat treatment, consisting of solution (4 h at 1423 K), stabilization (24 h at 1115 K) and γ' precipitation (20 h at 977 K). The overaging treatments were conducted subsequently, for times between 50 and 1000 h at 973 K (700 °C) and 1073 K (800 °C). While no special atmospheres were used in any treatment step, the analyzed cuts were made with 2 mm clearance from the surface as to guarantee the material integrity.

Lastly, analyses were conducted with scanning electron microscopy techniques (SE, EDS, EBSD), X-ray diffraction (XRD) and hardness measurement (HV). Grain sizes were determined by light microscopy in non-reinforced samples, and with the aid of EBSD analysis in the composites. The γ' particles diameter was estimated using SEM-SE images, after 20 random measurements in 5 different areas in each specimen. Chromium carbides and oxides were primarily characterized by EDS analysis, while other phases were identified after XRD analysis.

Results

After the initial heat-treatment, samples from the hot-rolled Inconel X-750 presented large grains, with an average diameter of $D_{\text{avg}} = 107 \pm 67 \mu\text{m}$. The same material produced through the HEM + SPS process, however, exhibited a much finer microstructure, having $D_{\text{avg}} = 4 \pm 1 \mu\text{m}$. When

analyzing the composites (Fig. 1), specimens produced by LEM + PS had grains with $D_{avg} = 9 \pm 4 \mu\text{m}$, while the composite produced by HEM + SPS presented $D_{avg} = 0.6 \pm 0.5 \mu\text{m}$.

Phases were also measured (Table 3), highlighting a significant increase in the chromium carbides size in composites produced by LEM + PS method after 1000 h of overaging at 1073 K. Likewise, chromium oxides were spotted both non-reinforced and composite forms produced by the HEM + PS route after the same treatment, though no changes in the state of chromium carbides were observed.

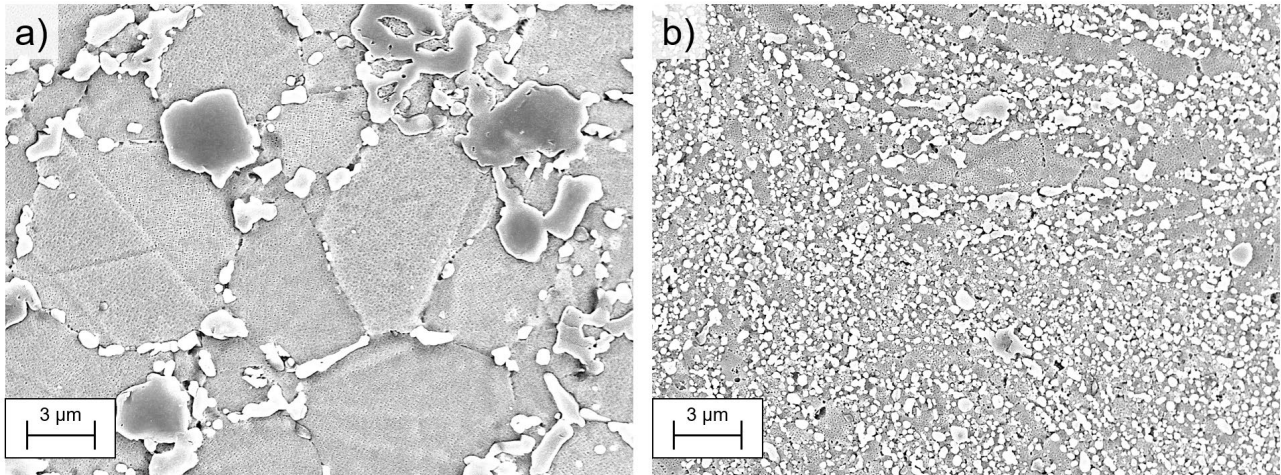


Fig. 1 - SEM images of composites at initial state, as produced by a) low energy milling + pressure sintering; b) high energy milling + spark plasma sintering.

The microstructure homogeneity was severely impaired on specimens produced by LEM + PS process, that presented TiC_p with $D_{avg} = 3.2 \pm 1 \mu\text{m}$ clustered at the original interface between the metallic powder particles. However, specimens prepared by the HEM process presented carbides with $D_{avg} = 0.3 \pm 0.1 \mu\text{m}$, a tenfold reduction in size. As a result, the TiC_p distribution in the matrix also improved significantly.

Table 3 - Average diameter* (μm) of carbides and oxides. Sensitive value changes are highlighted.

Material	Processing	Overaging	TiC	Cr_xC_y	Cr_xO_y
Inconel X-750 non-reinforced	Hot-rolling	Initial state	—	0.2	none
		After 1000 h at 1073 K	—	0.2	none
Inconel X-750 + TiC_p 15 vol.%	LEM + PS	Initial state	3.2	0.2	none
		After 1000 h at 1073 K	3.2	1.4	none
Inconel X-750 non-reinforced	HEM + SPS	Initial state	—	0.1	none
		After 1000 h at 1073 K	—	0.1	1.8
Inconel X-750 + TiC_p 15 vol.%	HEM + SPS	Initial state	0.3	n/d	0.8
		After 1000 h at 1073 K	0.3	n/d	1.9

* Measurement standard deviations: $\text{TiC} = \pm 0.1 \mu\text{m}$; $\text{Cr}_x\text{C}_y = \pm 0.4 \mu\text{m}$; $\text{Cr}_x\text{O}_y = \pm 0.3 \mu\text{m}$

A lath-shaped phase was observed in the Inconel X-750 produced by the HEM + SPS route (Fig. 2 c) at its initial state, having an average length of $5.3 \mu\text{m}$ and thickness of 65 nm . It was established as eta (η) phase, Ni_3Ti , through EDS and XRD analysis (Fig. 6). The areas surrounding these precipitates were depleted of γ' . Similar shaped laths, but present in significantly smaller amounts and with shorter length, were also noted in all other materials investigated in their initial state. This phase was further confirmed as η with the use of XRD analysis.

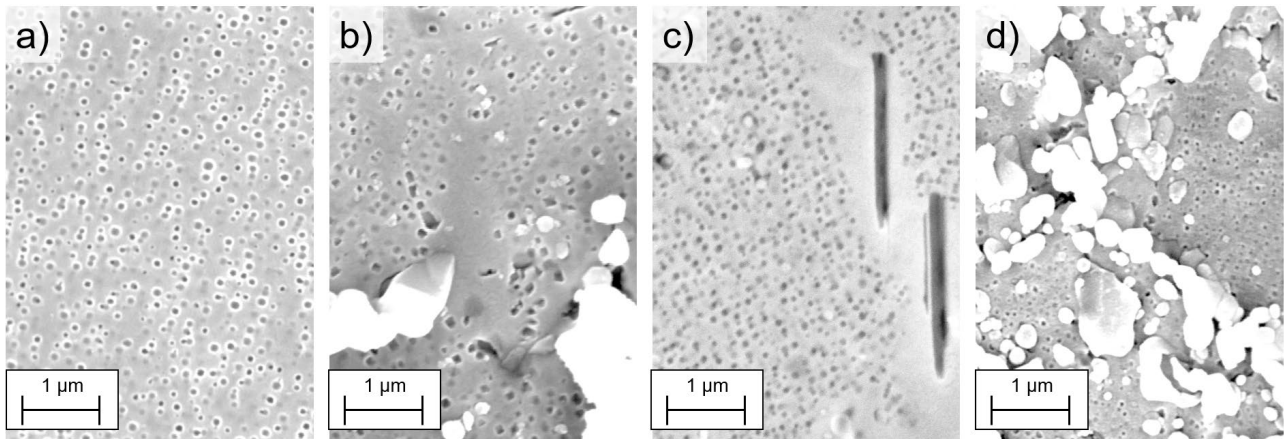


Fig. 2 - SEM images from samples in the initial state (as heat-treated): a) Inconel X-750 hot-rolled; b) X-750/TiC produced by low energy milling + PS; c) Inconel X-750 produced by SPS; d) X-750/TiC produced by high energy milling + SPS.

The laths of η phase identified in Inconel X-750 produced by HEM + SPS processes were also identified in specimens after exposure to 1073 K for 1000 h. The precipitate presented growth of 60% in average length, increasing from 5.3 to 8.4 μm .

γ' particles were identified on all materials evaluated (Fig. 2 and Fig. 3), at all overaging times. In samples produced by the HEM + SPS route, however, the γ' particle size was the smallest observed among all materials analyzed at their initial state (Fig. 4). Furthermore, after a 1000 h at 1073 K, these samples still showed a smaller γ' growth degree in comparison to materials produced through hot-rolling and traditional pressure sintering processes. It is worth noting that at 973 K specimens produced by LEM + PS method exhibited γ' particles shrinking with time. This decrease was accompanied by a loss of the original rounded-cuboidal form, with the particles becoming increasingly asymmetrical and less homogeneously distributed.

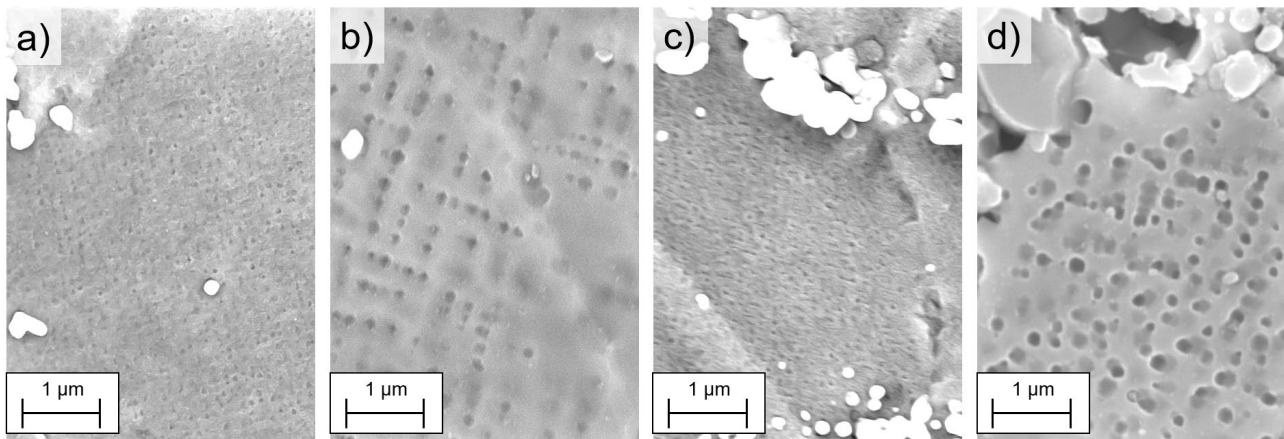


Fig. 3 - Composites after 1000 h of overaging. Specimens produced by low energy milling + PS, overaged at a) 973 K and b) 1073 K. Specimens produced by high energy milling + SPS, overaged at c) 973 K and d) 1073 K.

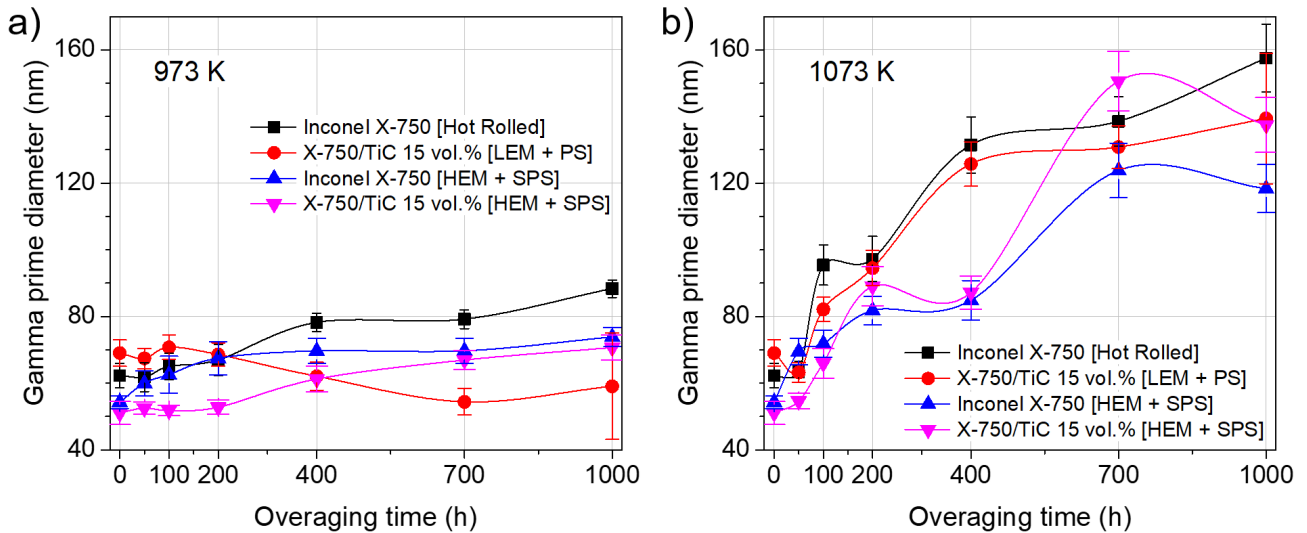


Fig. 4 - Average size of γ' particles, for specimens submitted to overaging at a) 973 K and b) 1073 K. Error bars represent the confidence interval, for $\alpha = 0.05$.

Through EDS punctual analysis on MC particles, it was determined that the Inconel X-750 samples in original state presented (Ti,Nb)C with an even Ti:Nb ratio, in addition to 9 at.% Cr. After being submitted to overaging for 1000 h at 973 K, their composition remained unchanged. However, specimens aged for 1000 h at 1073 K presented MC carbides enriched with Nb and Al, while having a reduced Cr content (1,6 at.%).

As expected, in the composite prepared by LEM + PS process the MC particles are Ti-rich, but they also presented similar small amounts of Nb and Cr after the initial heat-treatment. Following the 1000 h aging process, a strong Cr reduction was observed, from 3,95 at.% at treatment onset to 0,72 and 0,57 at.%, after aging at 973 and 1073 K, respectively. The composite produced by HEM + SPS method also exhibited MC particles enriched in Ti and Al, but exhibiting higher contents of Nb and Cr in comparison to pressure-sintered specimens.

While chromium oxides were spotted on the composite prepared by the HEM + SPS route already in samples at the original state, the volume of oxides more than doubled after 1000 h at 1073 K (Table 3). These were located mostly in the vicinity of larger chromium carbides (Fig. 5).

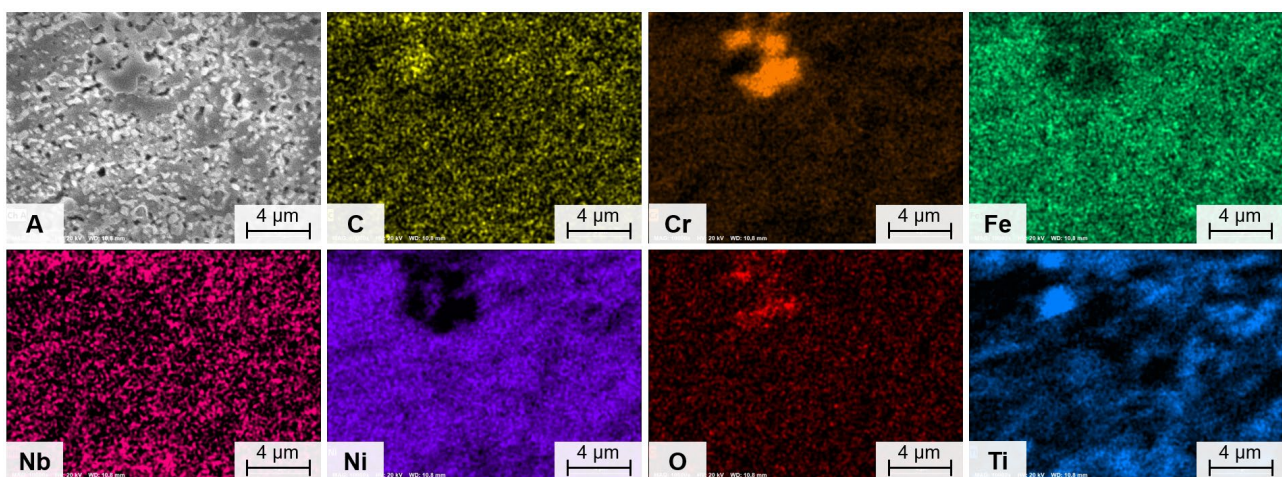


Fig. 5 - EDS elemental mapping of a specimen produced by HEM + SPS route, after being submitted to overaging for 1000 h at 1073 K.

Phases composing the microstructure were further determined by XRD analysis (Fig. 6). The composite prepared by LEM + PS process showed the presence γ and γ' , in addition to TiC, at all examined states: original and after 1000 h at both 973 and 1073 K. NbC was also detected on all analysis conducted. Specimens produced by HEM + SPS route exhibited the same phases, in addition

to η after 1000 h at 1073 K. Chromium carbides were not determined by XRD analysis, but only through EDS, since their major XRD peaks are concealed within peaks from more prevalent phases.

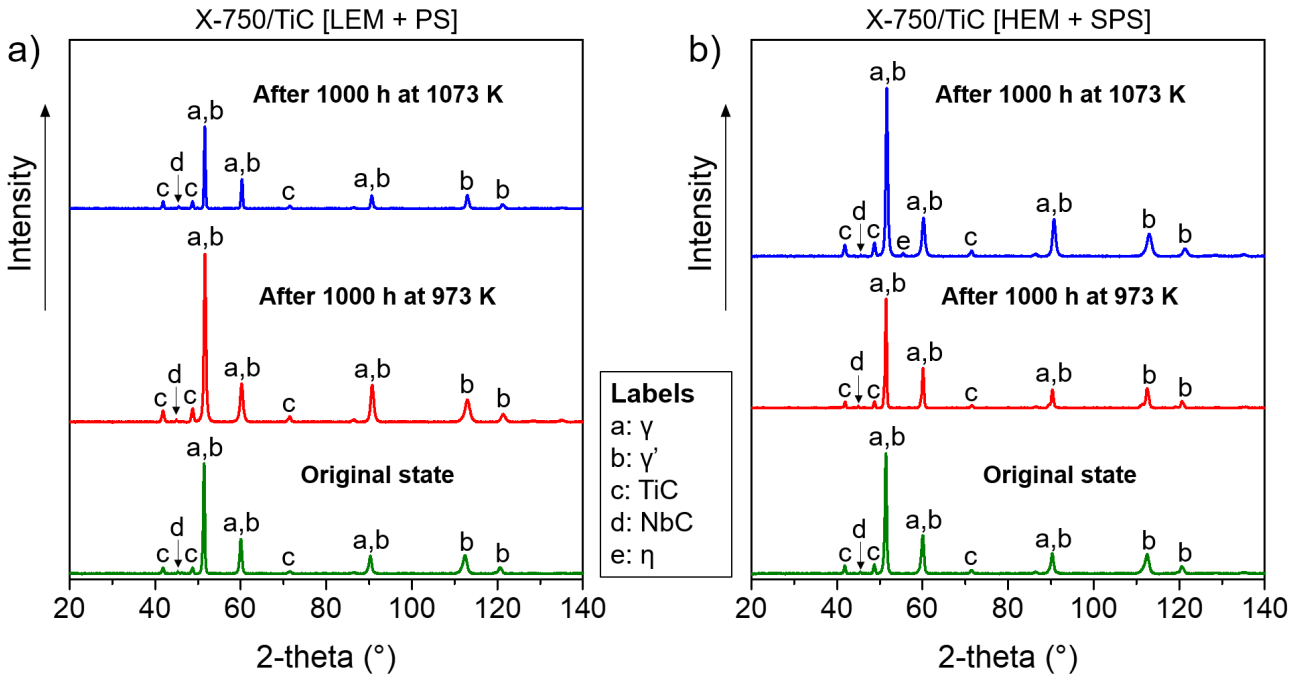


Fig. 6 - XRD diffractograms from composites produced by a) low energy milling + pressure sintering and b) high energy milling + spark plasma sintering.

Hardness measurements (Fig. 7) showed a notable decrease in the first 100 h of aging, on all specimens treated at 1073 K. The composite prepared by LEM + PS route, particularly, exhibited a strong decrease in hardness after 1000 h, for both tested temperatures. Contrary to these results, materials produced through HEM + SPS route exhibited the highest stability, presenting only minimal hardness changes between 100 and 1000 h of treatment.

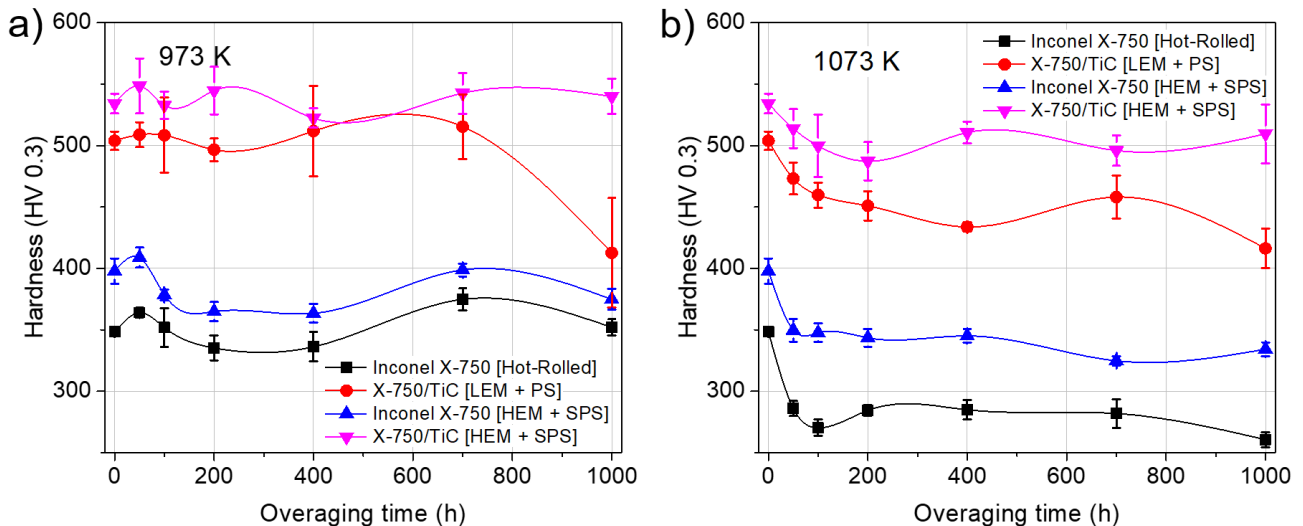


Fig. 7 - Average hardness evolution of specimens submitted to isothermal treatments conducted at a) 973 K and b) 1073 K. Error bars represent the confidence interval, for $\alpha = 0.05$.

A direct correlation can be established between the growth of γ' particles and the hardness decrease with time. The tendency is more evident in tests conducted at 1073 K, as shown by a comparison with composites prepared by different methods (Fig. 8). Specimens prepared by the LEM + PS route showed a stronger hardness loss during isothermal aging, accompanied by a trend of continuous γ' growth after the first 50 h of treatment.

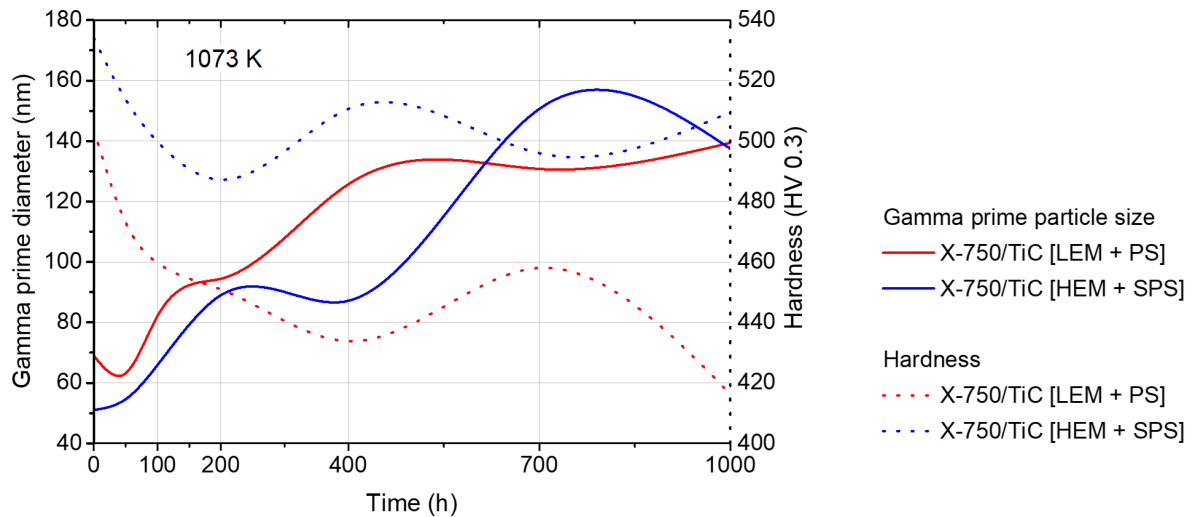


Fig. 8 - Polynomial fitting showing the correlation between γ' particle size and hardness, for composites submitted to isothermal treatments at 1073 K.

Discussion

Presenting a more homogeneous and refined microstructure, the composite prepared by the HEM + SPS route revealed a finer γ' dispersion at its initial state. It also showed higher stability during isothermal aging at 973 K, avoiding dissolution. When aged at 1073 K, it showed a similar growth of γ' particles after 1000 h, but maintaining mostly of the precipitate original morphology. The result can be attributed to the high energy milling process, that creates a finer dispersion of TiC_p . During the overaging process, Ti and Nb in solid solution diffuses to the MC phase nearby [6], as indicated by EDS punctual analysis on the Inconel X-750 over (Nb,Ti)C particles. Thus, it can be assumed that the availability of some elements that collaborate to γ' growth is also limited [6]. A near equilibrium situation during the isothermal aging, thereby, is potentially achieved.

A homogeneous distribution of γ' particles is essential to preserve the high creep resistance in the metallic matrix. Contrary to the non-reinforced alloy prepared by the HEM + SPS, the composite prepared through this route did not exhibit significant γ' -free zones. It can be assumed that in the former case a large amount of η phase led to a process of solute depletion in the area, thus improving the solubility around these particles and preventing the formation of γ' [8].

The SPS process provides a high localized heating, followed by a fast cooling step. As a result, a high amount of elements is kept in solid solution, inducing the formation of precipitates in an alternative order, when compared to processes with lower heating and cooling rates. A higher amount of Ti solubilized in the matrix, for instance, provides the driving force to the development of η phase in the non-reinforced alloy during the applied isothermal aging. Regarding the composite, however, that is not the case: it can be speculated that the fine dispersion of TiC_p resulting from the HEM + SPS processes promotes the diffusion of both Ti and Nb from the matrix to the carbides, reducing their availability to form phases such as Ni_3Ti and Ni_3Nb . Furthermore, γ' precipitates in the alloy Inconel X-750 are composed mostly by Ni_3Al , which seems unaffected by these changes in the composite.

The formation of hexagonal Ni_3Ti (η phase) is expected in turbine elements made of Inconel X-750 superalloy, after long time in service. The precipitate was identified in the composite prepared by the HEM + SPS process. If the presence of η is beneficial or detrimental to the material creep resistance, it is still subject of dispute. When fine distributed at grain boundaries, η may inhibit crack growth. However, its formation inside grains occurs at the expense of γ' [8], which has great importance to maintain the matrix strength.

Possible advantages regarding creep resistance on the composite produced by HEM + SPS are not limited to the achievement of a more stable and finer distribution of γ' . The material hardness evolution showed the lowest loss among all tested specimens, after 1000 h at 1073 K. It is known that the loss of coherency in overaged superalloys is linked to a softening process, in connection to creep resistance worsening [9].

Conclusions

A comprehensive analysis of selected Ni-based metal matrix composites and their non-reinforced counterparts submitted to long isothermal treatments was conducted. Specimens produced by a process of high energy milling, followed by spark plasma sintering, resulted in samples with the highest microstructural stability after the overaging treatments. A hypothesis is made that the partial diffusion of Ti and Nb from solid solution to nearby carbides collaborated to the higher stability situation in the matrix, limiting the growth of γ' precipitates. Moreover, no γ' -free zones were formed as a result of precipitation of an η phase in excess, contrary to the non-reinforced alloy produced by the same route.

The material produced by HEM + SPS method presented a homogeneous distribution of fine TiC particles, which combined with the highest γ' stability over long aging times at 973 K resulted in the lowest hardness loss among all investigated materials. The outcome suggests a potential for high creep resistance in the composite, when compared to the MMC prepared by the LEM + PS route.

Hexagonal Ni₃Ti (η phase) was observed after 1000 h of aging in specimens produced by the SPS process. While in the non-reinforced variety it caused the appearance of zones denuded of γ' , in the composite this phase was preserved. Further investigations to determine the influence of η in the creep resistance of Ni-based MMCs is, therefore, advised.

Acknowledgments

We thank the financial funding by the National Council for Scientific and Technological Development (CNPq, Brazil) and the Technische Hochschule Ingolstadt (THI, Germany).

References

- [1] G. Lemos, M. C. Fredel, F. Pyczak, and U. Tetzlaff, "Development of a TiC_p 15 vol.% Reinforced Ni-Based Superalloy MMC, with High Creep Resistance and Reduced Weight," *Key Eng. Mater.*, vol. 742, pp. 189–196, 2017.
- [2] J. S. Benjamin, "Mechanical alloying: A perspective," *Met. Powder Rep.*, vol. 45, no. 2, pp. 122–127, 1990.
- [3] M. Tokita, *Spark Plasma Sintering (SPS) Method, Systems, and Applications*, Second Ed. Elsevier Inc., 2013.
- [4] W. Yucheng and F. Zhengyi, "Study of temperature field in spark plasma sintering," *Mater. Sci. Eng. B Solid-State Mater. Adv. Technol.*, vol. 90, no. 1–2, pp. 34–37, 2002.
- [5] H. Hisazawa, Y. Terada, and M. Takeyama, "Morphology evolution of γ' precipitates during isothermal exposure in wrought Ni-based superalloy Inconel X-750," *Materials Transactions*, vol. 58, no. 5, pp. 817–824, 2017.
- [6] S. Floreen, G. E. Fuchs, and W. J. Yang, "The Metallurgy of Alloy 625," *Superalloys 718, 625, 706 Var. Deriv.*, pp. 13–37, 1994.
- [7] M. Sundararaman, P. Mukhopadhyay, and S. Banerjee, "Carbide Precipitation in Nickel Base Superalloys 718 and 625 and Their Effect on Mechanical Properties," *Superalloys 718, 625, 706 Var. Deriv.*, pp. 367–378, 1997.
- [8] G. D. Smith and S. J. Patel, "The Role of Niobium in Wrought Precipitation-Hardened Nickel-Base Alloys," *Superalloys 718, 625, 706 Var. Deriv.*, pp. 135–154, 2005.
- [9] M. Haël and U. Tetzlaff, "Microstructure and High-Temperature Strength of Monocrystalline Nickel-Base Superalloys," *Advanced Engineering Materials*, no. 6, pp. 319–326, 2000.